



## TeV gamma-rays from supernova remnants Tycho's SNR, Cas A, Crab and Geminga

V.G. SINITSYNA, S.I. NIKOLSKY, V.Y. SINITSYNA

*P.N. Lebedev Physical Institute, Leninsky pr. 53, Moscow, Russia*

[sinits@sci.lebedev.ru](mailto:sinits@sci.lebedev.ru)

DOI: 10.7529/ICRC2011/V07/0164

**Abstract:** Tycho's SNR has been observed by SHALON imaging Cherenkov telescope at Tien-Shan (3340 m a.s.l.). This object, Ia SNR, has long been considered as a candidate to CR hadron source in the Northern Hemisphere. The expected pion decay gamma-flux  $F_\gamma \sim E_\gamma^{-1}$  extends up to  $> 30$  TeV, whereas the IC gamma-ray flux has a cutoff above a few TeV. So, the detection of gamma-rays at energies of 10 - 80 TeV by SHALON is an evidence for hadron origin of the rays. The observation results on Cas A by SHALON are also presented. Its integral  $\gamma$ -ray flux at energies of  $> 0.8$  TeV is found to be  $(0.68 \pm 0.13) \times 10^{-12} \text{ cm}^{-2} \text{ s}^{-1}$  at energies of  $> 0.8$  TeV. The TeV photon spectrum measured by SHALON can be described with a power-law with the index of  $k_\gamma = -1.32 \pm 0.18$ . The value Geminga flux obtained by SHALON is lower than the upper limits published before by other experiments. Its integral  $\gamma$ -ray flux is found to be  $(0.48 \pm 0.10) \times 10^{-12} \text{ cm}^{-2} \text{ s}^{-1}$  at energies of  $> 0.8$  TeV. Within the range 0.8 - 6 TeV, the integral energy spectrum is well described by the power law  $I(> E_\gamma) \propto E_\gamma^{-0.59 \pm 0.10}$ . The energy spectrum of Geminga is harder than Crab spectrum. Crab Nebula has been regularly observed by high mountain SHALON telescope. The integral energy spectrum is well described by the power law  $I(> E_\gamma) \propto E_\gamma^{-1.40 \pm 0.07}$  within the range 0.8 - 30 TeV. An image of  $\gamma$ -ray emission from Crab Nebula by SHALON telescope is presented. TeV  $\gamma$ -quantum spectrum is generated by photons, produced by relativistic electrons and positrons via Inverse Compton if the average magnetic field in the region of VHE  $\gamma$ -ray emission 67 nT, which is taken from the comparison of TeV and X-ray emission regions (Chandra).

**Keywords:** Origin of Cosmic Rays, Supernova Remnants, Tycho's SNR, Cas A, Crab Nebula, Geminga.

## Introduction

The  $\gamma$ -quantum emitting objects in our Galaxy are the supernova remnants and binary. SNe of type Ib and II are more numerous in our Galaxy. TeV energies  $\gamma$ -rays, measurable by the imaging Cherenkov technique, are the most interesting for searching hadronic cosmic rays (CRs) in SNRs because they provide the information about CRs of highest possible energies  $10^{13} - 10^{14}$  eV. Direct information about high-energy CR population in SNRs can be obtained from  $\gamma$ -ray observation. According to the theoretical prediction about 20 SNRs should be visible in the TeV  $\gamma$ -rays some of them were detected by SHALON on Tien-Shan high-mountain station [1, 2, 3, 4, 5], namely Crab Nebula, Tycho's SNR, Cas A and Geminga.

## Crab Nebula

The Crab Nebula, most famous supernova remnant, plays an important role in the modern astrophysics. No other space object has such impact on the progress and development of the modern experimental and theoretical astrophysics methods. Pulsar located at the center of the Crab Nebula is the first whose optical, X-ray and  $\gamma$ -emission has been detected. Since the first detection with ground-based telescope the Crab has been observed by the num-

ber of independent groups using different methods of registration of  $\gamma$ -initiated showers. Some of these detections are presented below and shown on Fig. 1. The SHALON observation results of well-known  $\gamma$ -source Crab Nebula are presented at Figure 1 top in comparison with other experiments EGRET, COS-B, CELESTE, CAT, Asgat, Whipple, Themis, HEGRA CT2, CANGAROO, Tibet, CASA-MIA. The spectrum of  $\gamma$  rays from the Crab Nebula has been measured in the energy range 0.8 TeV to 30 TeV at the SHALON Alatoo Observatory by the atmospheric Cherenkov technique with a statistical significance of 36.1 $\sigma$ [6]. The integral energy spectrum is well described by the single power law  $I(> E_\gamma) \propto E_\gamma^{-1.40 \pm 0.07}$  (Fig. 1 top).

Crab Nebula has an extraordinary broad spectrum, attributed to synchrotron radiation of electrons with energies from GeV to PeV. This continuous spectrum appears to terminate near  $10^8$  eV and photons, produced by relativistic electrons and positrons ( $\sim 10^{15}$  eV) via Inverse Compton, form a new component of spectrum in GeV - TeV energy range. To make a description of the intensity and spectral shape in the TeV region of  $> 0.8$  TeV, the model of inverse Compton scattering of the ambient photons in the nebula in the Ref. [10] is used.

For the purpose of calculating the Inverse Compton scattered radiation, the complete spectrum of Crab Nebula need

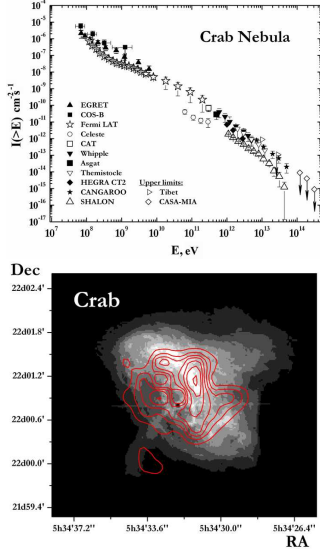


Figure 1: **top** – The Crab Nebula  $\gamma$ -quantum integral spectrum by SHALON [1, 2, 3, 4, 5] in comparison with other experiments: Fermi LAT, EGRET, COS-B, CELESTE, CAT, Asgart, Whipple, Themisocle, HEGRA CT2, CANGAROO, Tibet, CASA-MIA [7, 8, 9, 10, 11, 12, 13, 14, 15]; **bottom** – A Chandra X-ray image of Crab Nebula [17]. The central part  $200'' \times 200''$  of Crab Pulsar Wind Nebula (PWN) in the energy range 0.2–4 keV. The contour lines show the TeV - structure by SHALON observations.

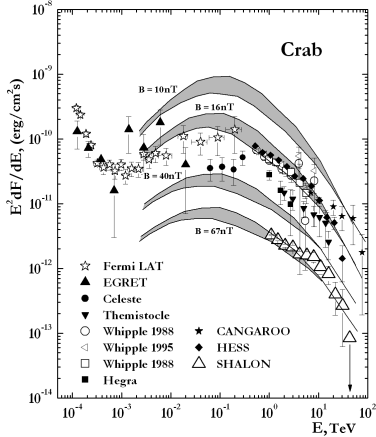


Figure 2: The Crab Nebula  $\gamma$ -quantum spectrum by SHALON together with other experiments [4, 7, 8, 9, 10, 11, 12, 13, 14, 16, 15]: Fermi, Celeste, Whipple, EGRET, CANGAROO, HEGRA, Magic, HESS and with the predicted inverse Compton spectrum for the different field strengths [10] and for the 67 nT.

to be taken into account to deduce the spectrum of relativistic electrons [10]. Additionally, we need the assuming about magnetic field strength in the region of emission (Figs. 1). The average magnetic field in the region of VHE  $\gamma$ -ray emission is extracted from the comparison of 0.8 – 30 TeV (SHALON data) and X-ray (Chandra data [17]) emission regions. In order to find relation between

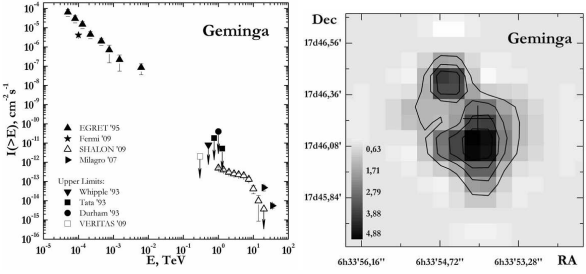


Figure 3: **left:** The Geminga  $\gamma$  - quantum ( $E > 0.8$  TeV) integral spectrum by SHALON in comparison with other experiments EGRET, Fermi LAT [23], Milagro [22] and upper limits: Whipple'93 [18], Tata'93 [19], Durham'93 [20] and Veritas [21]; **right:** The image of  $\gamma$ -ray emission from SHALON.

TeV and X-ray emission and characteristics which are necessary to calculate a VHE  $\gamma$ -ray spectrum, the combination of SHALON and Chandra images were analyzed.

Figure 1 presents a Chandra X-ray image of the central part  $200'' \times 200''$  of Crab Nebula in the energy range 0.2 – 4 keV. In this energy band most of the PWN X-rays come from a torus surrounding the pulsar. The contour lines show the TeV - structure by SHALON observations. The most part of TeV energy  $\gamma$ -quanta come from the region of bright torus (see Fig. 1). Magnetic fields and lifetimes of representative regions in Chandra image of Crab have been derived [17] and ranges from 6.2 up to 15.3 nT.

The TeV  $\gamma$ -quantum spectrum of Crab by SHALON is generated via Inverse Compton of soft, mainly optical, photons which are produced by relativistic electrons and positrons, in the nebula region around  $1.5'$  (see Figs. 1 and 2) from the pulsar with specific average magnetic field of about 67 nT.

## Geminga

A neutron star in the constellation Gemini is the second brightest source of high-energy  $\gamma$ -rays in the sky, discovered in 1972, by the SAS-2 satellite. For nearly 20 years, the nature of Geminga was unknown, since it didn't seem to show up at any other wavelengths. In 1991, an regular periodicity of 0.237 second was detected by the ROSAT satellite in soft X-ray emission, indicating that Geminga is almost certainly a pulsar. Geminga is the closest known pulsar to Earth.

Geminga is one of the brightest source of MeV - GeV  $\gamma$ -ray, but the only known pulsar that is radio-quiet. Geminga has been the object for study at TeV energies with upper limits being reported by three experiments Whipple'93 [18], Tata'93 [19], Durham'93 [20] and very recently by VERITAS [21]. Also Geminga has observed with Milagro [22] at energies of 20 TeV and 35 TeV and Fermi LAT at energies 30 MeV - 200 GeV [23]. The spectrum by Fermi is fitted with a power law with exponential cutoff in the form:  $dN/dE = N_0 \times (E^{-\gamma}) \exp(-E/E_0)$ , where  $N_0 = (1.19 \pm 0.08) \times 10^{-6} \text{ GeV}^{-1} \text{ cm}^{-2} \text{ s}^{-1}$ ,  $\gamma = 1.3 \pm 0.05$ ,  $E_0 = (2.47 \pm 0.19) \text{ GeV}$ .

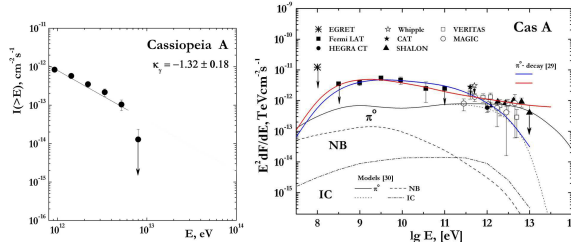


Figure 4: **left:** The Cas A  $\gamma$ -quantum integral spectrum with power index of  $k_\gamma = -1.32 \pm 0.18$  by SHALON experiment; **right:** Spectral energy distribution of the  $\gamma$ -ray emission from Cas A (see text).

Figure 3 shows the SHALON results for this  $\gamma$ -source [1, 2, 3, 4, 5]. An image of  $\gamma$ -ray emission from Geminga by SHALON telescope is shown in Fig. 3. As is seen from this figure the value Geminga flux obtained by SHALON is lower than the upper limits published before. Its integral  $\gamma$ -ray flux is found to be  $(0.48 \pm 0.10) \times 10^{-12} \text{ cm}^{-2} \text{ s}^{-1}$  at energies of  $> 0.8 \text{ TeV}$  [1] with a significance of  $7.4\sigma$  [6]. Within the range  $0.8 - 6 \text{ TeV}$ , the integral energy spectrum is well described by the single power law  $I(> E_\gamma) \propto E_\gamma^{-0.59 \pm 0.10}$  (Fig. 3). The energy spectrum of supernova remnant Geminga  $F(E_O > 0.8 \text{ TeV}) \propto E^k$  is harder than Crab spectrum.

## Cassiopeia A

Cassiopeia A (Cas A) is the youngest of historical supernova remnant in our Galaxy. The supernova explosion that gave rise to Cas A occurred around 1680. Its overall brightness across the electromagnetic spectrum makes it a unique object for studying high-energy phenomena in SNRs. Cas A was detected in TeV  $\gamma$  rays, first by HEGRA [24] and later confirmed by MAGIC [25] and VERITAS [26]. The high energy  $\gamma$ -ray emission from Cas A was detected with Fermi LAT [27] in the range 500 MeV - 50 GeV.

Cas A was observed with SHALON telescope during the 27 hours of autumn 2010 [5]. All observations were made with the standard procedure of SHALON experiment during moonless nights. The  $\gamma$ -ray source associated with the SNR Cassiopeia A was detected above 800 GeV with a statistical significance of  $7.1\sigma$  [6] with a  $\gamma$ -quantum flux above 0.8 TeV of  $I_{\text{CasA}}(> 0.8 \text{ TeV}) = (0.68 \pm 0.13) \times 10^{-12} \text{ cm}^{-2} \text{ s}^{-1}$ . The  $\gamma$ -ray integral spectrum is presented in fig. It is compatible with a power law with an index  $k_\gamma = 1.32 \pm 0.18$ .

The favored scenarios in which the  $\gamma$ -rays of 500 MeV - 10 TeV energies are emitted in the shell of the SNR like Cas A are considered in [27], [28]. The  $\gamma$ -ray emission could be produced by electrons accelerated at the forward shock through relativistic bremsstrahlung (NB) or IC [27]. Alternatively, the GeV  $\gamma$ -ray emission could be produced by accelerated CR hadrons through interaction with the background gas and then  $\pi^0$ -decay. Figure 4 presents spectral energy distribution of the  $\gamma$ -ray emission from Cas A by

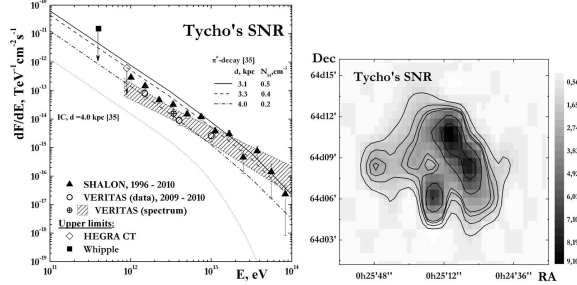


Figure 5: **left:** The Tycho's SNR  $\gamma$ -ray differential spectrum by SHALON in comparison with VERITAS data [32] and theoretical models [33, 34]; **right:** The SHALON image of  $\gamma$ -ray emission from Tycho's SNR.

SHALON in comparison with other experiment data Fermi LAT [27], HEGRA [24], MAGIC [25], VERITAS [26], EGRET [29], CAT [30], Whipple [31] and with theoretical predictions [27], [28]. Solid lines show the very high energy  $\gamma$ -ray spectra of hadronic origin. Dash-and-dot line presents the  $\gamma$ -ray spectrum of the IC emission [27]. The leptonic model with  $B = 0.12 \text{ mG}$  and  $B = 0.3 \text{ mG}$  also proposed in [27]. It was shown that leptonic model with  $B = 0.3 \text{ mG}$  predicts a 5 - 8 times lower  $\gamma$ -ray flux than the observed; the model with  $B = 0.12 \text{ mG}$ , which can broadly explain the observed GeV flux predicts the TeV spectrum with cut-off energy about 10 TeV. The detection of very high energy  $\gamma$ -ray emission at 5 - 10 TeV and the hard spectrum below 1 GeV would favor the  $\pi^0$ -decay origin of the  $\gamma$ -rays in Cas A SNR.

## Tycho's SNR

Tycho Brage supernova remnant has been observed by SHALON atmospheric Cherenkov telescope of Tien-Shan high-mountain observatory. This object has long been considered as a candidate to cosmic ray hadrons source in Northern Hemisphere, although it seemed that the sensitivity of the present generation of Imaging Atmospheric Cherenkov System's too small for Tycho's detection. Tycho's SNR has been detected by SHALON at TeV energies [1, 2, 3, 4, 5] with a statistical significance of  $17\sigma$  [6]. The integral  $\gamma$ -ray flux above 0.8 TeV was estimated as  $(0.52 \pm 0.05) \times 10^{-12}$  (Fig. 6). Figures 6 and 5 show the observational results for the Tycho's SNR. An image of  $\gamma$ -ray emission from Tycho's SNR by SHALON telescope is shown in Fig. 5. The energy spectrum of Tycho's SNR at  $0.8 - 20 \text{ TeV}$  can be approximated by the power law  $F(> E_O) \propto E^{k_\gamma}$ , with  $k_\gamma = -0.96 \pm 0.06$ . The energy spectrum of supernova remnant Tycho's SNR  $F(E_O > 0.8 \text{ TeV}) \propto E^k$  is also harder than Crab spectrum.

Recently, Tycho's SNR was also confirmed with VERITAS [32] telescope in observations of 2008 - 2010 years. Figure 5 presents the Tycho's SNR differential spectrum by SHALON comparing with VERITAS [32] data and theoretical models [33, 34].

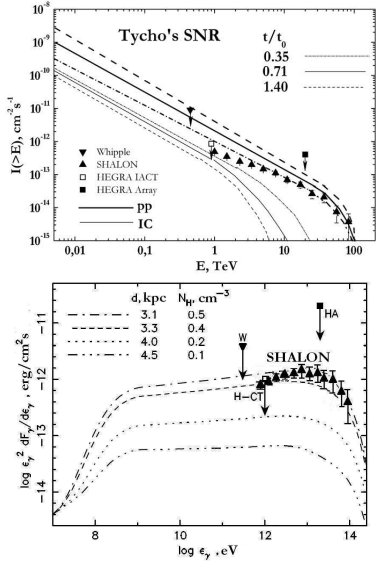


Figure 6: **top:** The Tycho's SNR  $\gamma$ -ray spectrum by SHALON in comparison with other experiments: the observed upper limits Whipple, HEGRA IACT system, HEGRA AIROBICC and calculations: IC emission (thin lines),  $\pi^0$  - decay (thick lines) [33]. **bottom:** Spectral energy distribution of the  $\gamma$ -ray emission from Tycho's SNR [36, 37]. All cases have dominant hadronic  $\gamma$ -ray flux.

A nonlinear kinetic model of cosmic ray acceleration in supernova remnants is used in [33, 34] (Fig. 6), to describe the properties of Tycho's SNR. The  $\pi^0$ -decay  $\gamma$ -quantum flux turns out to be some greater than inverse Compton flux at 1 TeV becomes strongly dominating at 10 TeV. The predicted  $\gamma$ -quanta flux is in consistent with upper limits published by Whipple [7, 8, 35] and HEGRA [9]. The expected flux of  $\gamma$ -quanta from  $\pi^0$ -decay,  $F_\gamma \propto E_\gamma^{-1}$ , extends up to  $\sim 30$  TeV, while the flux of  $\gamma$ -rays originated from the Inverse Compton scattering has a sharp cutoff above the few TeV, so the detection of  $\gamma$ -rays with energies of  $\sim 10$  to 80 TeV by SHALON is an evidence of their hadronic origin [33, 36, 37]. Figure 6 presents spectral energy distribution of the  $\gamma$ -ray emission from Tycho's SNR, as a function of  $\gamma$ -ray energy  $\epsilon_\gamma$ , for a mechanical SN explosion energy of  $E_{SN} = 1.2 \times 10^{51}$  erg and four different distances  $d$  and corresponding values of the interstellar medium number densities  $N_H$ . All cases have dominant hadronic  $\gamma$ -ray flux [37]. The additional information about parameters of Tycho's SNR can be predicted in frame of nonlinear kinetic model [33, 36, 37] if the TeV  $\gamma$ - quantum spectrum of SHALON telescope is taken into account: a source distance 3.1 - 3.3 kpc and an ambient density  $N_H$   $0.5 - 0.4 \text{ cm}^{-3}$  and the expected  $\pi^0$ -decay  $\gamma$ -ray energy spectrum extends up to about 100 TeV.

## References

- [1] V. G. Sinitzyna, AIP Conf. Proc., 1999, **515**: 205, 293.
- [2] V. G. Sinitzyna, S. I. Nikolsky, *et al.*, Izv. Ross. Akad. Nauk Ser. Fiz., 2002, **66**(11): 1654 and 1661; *ibid.* 2005, **69**(3): 422.
- [3] V. G. Sinitzyna, *et al.*, in Proc. of 27th ICRC, Hamburg, 2001, **3**: 2665; of 29th ICRC, Puna, 2005, **4**: 231; of 30th ICRC, Merida, 2007, **2**: 543.
- [4] V. G. Sinitzyna *et al.*, Nucl. Phys. B (Proc. Suppl.), 2009 **196**: 437; *ibid.*, 2008 **175-176**: 455; *ibid.*, 2006, **151**: 112; *ibid.*, 2003, **122**: 247, 409; *ibid.*, 2001 **97**: 215 and 219; *ibid.*, 1999 **75A**: 352.
- [5] V. G. Sinitzyna and V. Yu. Sinitzyna Pisma v Astronomicheskii Zhurnal, 2011, **37**(8): 1 - 15.
- [6] T.-P. Li and Y.-Q. Ma, Astrophys. J., 1983, **272**: 317.
- [7] T. C. Weekes, AIP Conf. Proc., 1999, **515**: 3.
- [8] M. Catanese & T.C. Weekes, 1999, Prep. Ser., No4811.
- [9] J. Prahla and C. Prosch (for the HEGRA Collaboration), in Proc. 25th ICRC, Durban, 1997, **3**: 217.
- [10] A. M. Hillas, *et al.*, ApJ, 1998, **503**: 744.
- [11] T. Tanimori, *et al.*, ApJ, 1998, **492**: 133.
- [12] F. Piron, *et al.*, in Proc. 28th ICRC, Tsukuba, 2003: 2607.
- [13] F. Aharonian, *et al.* ApJ, 2000, **539**: 317.
- [14] C. Masterson, *et al.*, in Proc. 29th ICRC, Puna, 2005, **4**: 143.
- [15] A. A. Abdo, *et al.*, ApJ, 2010, **708**: 1254.
- [16] R. M. Wagner, *et al.*, in Proc. 29th ICRC, Puna, 2005, **4**: 163.
- [17] F. D. Seward, W. H. Tucker and R. A. Fesen, ApJ., 2006, **652**: 1277.
- [18] C. W. Akerlof *et al.* in Proc. 23rd ICRC, Calgary, 1993, **1**: 305.
- [19] P. R. Vishwanath *et al.* A&A, 1993, **267**: L5.
- [20] C. C. G. Bowden *et al.* J. Phys. G: Nucl. Part. Phys., 1993, **19**: L29-L31.
- [21] G. Finnegan; Proc. of the 31st ICRC, Lodz 2009;
- [22] A. A. Ado *et al.* *arXiv:0904.1018v1*; *arXiv:0705.0707v1*;
- [23] O. Celik; Proc. of the 31st ICRC, Lodz 2009;
- [24] F. Aharonian, *et al.*, Astron. Astrophys. 2001, **370**: 112.
- [25] J. Albert *et al.*, Astron. Astrophys., 2007, **474**: 937.
- [26] V. A. Acciari, *et al.*, Astrophys. J., 2010, **714**: 163.
- [27] A.A. Abdo, *et al.*, Astrophys. J., 2010, **710**: L92.
- [28] E. G. Berezhko, G. Pühlhofer, H. J. Völk, Astron. Astrophys., 2003, **400**: 971.
- [29] J. A. Esposito *et al.*, Astrophys. J., 1996, **461**: 820.
- [30] P. Goret, *et al.*, Proc. of 26th ICRC, (Ed. D. Kieda, M. Salamon, B. Dingus), 1999, **3**: 496.
- [31] R. W. Lessard, *et al.*, Proc. of 26th ICRC, (Ed. D. Kieda, M. Salamon, B. Dingus), 1999, **3**: 488.
- [32] V. A. Acciari *et al.* *arXiv:astroph/1102.3871v1*
- [33] H. J. Völk, E. G. Berezhko, *et al.*, in Proc. 27th ICRC, Hamburg, 2001, **2**: 2469.
- [34] E. G. Berezhko, L. T. Ksenofontov and H. J. Völk, *Astrophys. Space Sci.*, 2007, **309**: 385.
- [35] J. H. Buckley, C. W. Akerlof, D. A. Carter-Lewis, *et al.*, Astron. Astrophys., 1998, **329**: 639.
- [36] H. J. Völk, E. G. Berezhko and L. T. Ksenofontov, in Proc. 29th ICRC, Pune, 2005, **3**: 235.
- [37] H. J. Völk, E. G. Berezhko, L. T. Ksenofontov *Astron.&Astrophys.*, 2008, **483**(2): 529.